Journal of Histochemistry & Cytochemistry 2016, Vol. 64(3) 190–204

DOI: 10.1369/0022155415627679
jhc.sagepub.com
SAGE

Stem Cell-Associated Marker Expression in Canine Hair Follicles

Nora M. Gerhards, Beyza S. Sayar, Francesco C. Origgi, Arnaud Galichet, Eliane J. Müller, Monika M. Welle[1], and Dominique J. Wiener[1]

Institute of Animal Pathology, Dermfocus, Vetsuisse Faculty (NMG, BSS, AG, EJM, MMW, DJW), Molecular Dermatology and Stem Cell Research, Institute of Animal Pathology and DermFocus, Vetsuisse Faculty (BSS, AG, EJM), Center for Fish and Wildlife Medicine, Vetsuisse Faculty (FCO), and Department of Dermatology, Inselspital, Bern University Hospital (EJM), University of Bern, Bern, Switzerland

Summary

Functional hair follicle (HF) stem cells (SCs) are crucial to maintain the constant recurring growth of hair. In mice and humans, SC subpopulations with different biomarker expression profiles have been identified in discrete anatomic compartments of the HF. The rare studies investigating canine HF SCs have shown similarities in biomarker expression profiles to that of mouse and human SCs. The aim of our study was to broaden the current repertoire of SC-associated markers and their expression patterns in the dog. We combined analyses on the expression levels of *CD34, K15, Sox9, CD200, Nestin, LGR5* and *LGR6* in canine skin using RT-qPCR, the corresponding proteins in dog skin lysates, and their expression patterns in canine HFs using immunohistochemistry. Using validated antibodies, we were able to define the location of CD34, Sox9, Keratin15, LGR5 and Nestin in canine HFs and confirm that all tested biomarkers are expressed in canine skin. Our results show similarities between the expression profile of canine, human and mouse HF SC markers. This repertoire of biomarkers will allow us to conduct functional studies and investigate alterations in the canine SC compartment of different diseases, like alopecia or skin cancer with the possibility to extend relevant findings to human patients. (J Histochem Cytochem 64:190–204, 2016)

Keywords

Stem cells, canine, hair follicle, immunohistochemistry

Introduction

The hair follicle (HF) undergoes recurrent phases of controlled growth (anagen), regression of the lower follicle (catagen) and relative quiescence (telogen), which, under healthy conditions, lasts throughout lifetime. This process is similar in mice, humans and dogs, and is initiated by HF stem cell (SC) activation. Major SC subpopulations of the HF are located in the isthmus, which begins at the opening of the sebaceous gland duct and ends at the insertion point of the arrector pili muscle (Purba et al. 2014). The isthmus includes the bulge, defined in mice as the follicular SC-bearing region at the attachment site of the arrector pili muscle at the bottom of the permanent portion (Watt and Jensen 2009). The area above the isthmus up to the opening of the HF to the outside is called the infundibulum, and the area below, comprising the distal part of the HF in the anagen hair cycle (HC) stage, is the inferior portion. The inferior portion can be further subdivided in the bulbar and the suprabulbar regions (Schneider et al. 2009). In contrast to the segment formed by the isthmus and the infundibulum, which is permanent, the inferior portion is transitional; it is only present in anagen and undergoes recurrent regression during catagen and is absent in telogen HC stages. In telogen HFs, a secondary hair germ is formed directly above

Received for publication July 15, 2015; accepted December 28, 2015.

[1]These authors contributed equally to this work

Corresponding Author:
Dominique J. Wiener, Institute of Animal Pathology, Dermfocus, Vetsuisse Faculty, University of Bern, Länggassstrasse 122, Bern, 3012, Switzerland.
Email: dominique.wiener@vetsuisse.unibe.ch

the dermal papilla at the lowermost part of the HF. It initiates a new HC at the end of the resting telogen phase (Greco et al. 2009).

The dog has, like other carnivores (e.g., cats), compound hair follicles. A follicular compound consists of a group of up to 15 hair follicles in which each infundibulum contains multiple hair shafts. In these groups, a large central primary hair is surrounded by up to five smaller lateral primary hairs, which are the guard hairs. The primary hairs are surrounded by smaller secondary hairs ("down", "wool", "undercoat") (Scott et al. 2001; Meyer 2009; Maxie 2015). In contrast to the carnivore hair follicle anatomy, most omnivores and herbivores (horses, cattle, pigs, rats, and mice, for example) have simple follicles that are not grouped and each infundibulum contains only one hair shaft. Humans and sheep have, depending on the body location, simple or compound follicles. In the human scalp, most follicular units are composed of two to four hairs whereas, on the body, simple HFs are present (Pinkus 1951; Meyer 2009).

SCs are located in a unique microenvironment consisting of neighboring cells, molecular signals and extracellular matrix, collectively forming the SC niche (Rompolas and Greco 2014). They are "slow-cycling", relatively undifferentiated multipotent cells with the ability to exit their quiescent status to generate a new HF via transient amplifying cells. Transient amplifying cells differentiate into all components of the new HF, including the hair shaft, in response to appropriate growth stimuli (Hsu et al. 2014). SCs, their location, marker expression and function have been extensively studied in the mouse (Rompolas and Greco 2014). However, relatively little is known in humans and even less in the dog (Kobayashi et al. 2010; Purba et al. 2014). In mice and humans, several distinct SC subpopulations in anatomic discrete compartments have been identified (Inoue et al. 2009; Arwert et al. 2012; Watt 2014), and it is noteworthy that anatomic and functional differences exist between species (Purba et al. 2014).

For our study, we selected the following early SC or progenitor cell markers with functional relevance based on murine, human and canine data: CD34, Sox9, keratin 15 (K15), leucine-rich repeat-containing G protein-coupled receptor 5 (LGR5), Nestin, leucine-rich repeat-containing G protein-coupled receptor 6 (LGR6) and CD200 (Lyle et al. 1998; Li et al. 2003; Liu et al. 2003; Trempus et al. 2003; Vidal et al. 2005; Ohyama et al. 2006; Jaks et al. 2008; Snippert et al. 2010).

The transmembrane glycoprotein CD34 is a well-established marker for murine bulge cells. It has been previously shown that CD34+ cells have label-retaining properties and a large proliferative potential in vivo (Trempus et al. 2003).

The transcription factor Sox9 is a sex-determining gene and its role in hair development and maintenance was introduced by Vidal et al. (2005). Another study showed that Sox9 plays a striking role in SC specification in mice, and its deletion diminishes the maintenance of bulge SCs (Nowak et al. 2008). Sox9 expression is mediated by sonic hedgehog signaling, an important morphogen involved in HF morphogenesis and anagen induction (Fantauzzo et al. 2012).

K15, a type I keratin protein, is well described as a marker of cells with SC properties in the HF and the epidermis; although, in the strictest sense, K15 is rather involved in early keratinocyte differentiation in humans, mice and dogs (Lyle et al. 1998; Liu et al. 2003; Kobayashi et al. 2009).

LGR5 is a transmembrane-domain receptor, introduced as a marker of rapidly cycling SCs in the small intestine and colon (Barker et al. 2007). Jaks et al. (2008) detected the expression of LGR5 in murine HFs. The presence of LGR5 mRNA was also demonstrated in human bulge cells (Garza et al. 2011). Lineage-tracing assays revealed that K15+ cells originate from Lgr5+ cells (da Silva-Diz et al. 2013).

Nestin, a class VI intermediate filament protein, was originally identified as a marker of neuronal stem and progenitor cells. In murine outer root sheath (ORS) cells, its expression was demonstrated by Li et al. (2003). In humans, Nestin highlights the mesenchymal SC component of the folliculosebaceous-apocrine unit rather than identifying the keratinocyte SCs (Sellheyer et al. 2011).

LGR6+ cells are considered, to date, as the most primitive epidermal SC population in adult murine HFs, and are located in the central isthmus directly above the bulge of murine HFs (Snippert et al. 2010; Rishikaysh et al. 2014). It has been shown that LGR6+ cells give rise to LGR5+ cells and contribute to HF regeneration (Rishikaysh et al. 2014).

CD200 is a type-1 transmembrane glycoprotein used for the enrichment of living human bulge cells (Ohyama et al. 2006). CD200 is not solely expressed in the bulge but also in the secondary germ and weakly in the sub-bulge area (Inoue et al. 2009; Garza et al. 2011).

In mice, the isthmus contains cells expressing CD34, K15 and LGR6 during all HC stages and Sox9 and Nestin during anagen stages (Li et al. 2003; Liu et al. 2003; Trempus et al. 2003; Vidal et al. 2005; Snippert et al. 2010). In murine anagen HFs, Sox9-positive cells are abundant in the ORS; however, in the lower part of the HF, ORS cells lack Sox9 expression. In telogen, a small number of cells are Sox9-positive at the base of the follicle epithelium (Vidal et al. 2005). LGR5+ cells are present in the secondary hair germ and the lower ORS of murine telogen HFs as well as in the ORS of the suprabulbar and the bulbar region of anagen HFs (Jaks et al. 2008). Nestin expression in mice is not restricted to the isthmus but extends to the inferior portion during anagen (Li et al. 2003). CD200 is predominantly located in the outermost layer of the ORS throughout the length of the anagen HF and does not localize to the bulge area (Rosenblum et al. 2004).

CD34 and K15 are prominent examples of interspecies differences between mice and humans. These markers are uniquely located in the bulge in mice. In humans, K15

expression is not limited to the bulge but is present in the entire isthmus according to most publications and one study reported K15 expression also in the suprabulbar region. Published results vary depending on the antibody used (Kloepper et al. 2008; Purba et al. 2014). In contrast to the mouse, CD34-expressing cells were found in humans in the proximal part of the isthmus and the suprabulbar ORS in anagen (Kloepper et al. 2008; Purba et al. 2014). This difference may partially be explained by the less dense structure of the human bulge involving a larger part of the isthmus as compared to the compact murine bulge, which is co-located at the insertion site of the arrector pili muscle and is visible as a trochanter-like projection. Other markers, such as Sox9, show the same expression pattern in humans and mice (Krahl and Sellheyer 2010). LGR5 protein expression has, to the best of our knowledge, not been investigated in human HFs. Nestin expression was described in the dermal papilla and the connective tissue sheath of human anagen HFs, suggesting its role as a marker of mesenchymal progenitor cells (Sellheyer et al. 2011). Cells expressing LGR6 have been detected in the entire ORS of human HFs (Wu et al. 2014) and CD200 is expressed by human anagen bulge cells (Ohyama et al. 2006).

In dogs, the characteristics of HF SCs and their progeny are still ill-defined. Only few studies investigating SC-related biomarker expression have been published and these are somewhat conflicting. Using frozen sections, one study reported that CD34 immunoreactivity is diffusely present in the ORS of the entire follicular isthmus (Kobayashi et al. 2009). In that study, the cycle stage of the investigated HFs was not noted. In another study, CD34 expression was restricted to the basal layer of the isthmus at all HC stages (Pascucci et al. 2006). The presence of canine Sox9 mRNA has been described, and was determined to be highest in the bulge area (Kobayashi et al. 2010); the location of Sox9 protein within the canine HF has not been determined. In one study, K15 expression was observed in the entire ORS of the isthmus of canine HFs near the insertion point of the arrector pili muscle (Brachelente et al. 2013), and, in two other studies, it was found in the outermost layer of the ORS between the insertion point of the arrector pili muscle and the sebaceous gland, which, in dogs, corresponds to the entire isthmus (Kobayashi et al. 2009; Kobayashi et al. 2010). The expression of Nestin was demonstrated in the isthmus of canine primary HFs (Mercati et al. 2008).

As non-inflammatory alopecia associated with HC arrest is a common complaint in dogs and because follicular SCs are essential for maintaining the HC, the aim of our study was to extend upon the current knowledge of the canine SC compartment with respect to known SC-associated marker expression. Due to the similarities in HF morphology, hair types, HC and the occurrence of analogous alopecic disorders in different dog breeds and in humans, the dog is also a promising model for comparative studies with human diseases. Detailed knowledge about the canine HF SC compartment could facilitate valuable investigations with respect to human alopecia, skin cancer and regenerative medicine.

Material & Methods

Skin Biopsies

Eight mm punch skin biopsies were obtained from ten healthy beagles, euthanized for reasons that were not related to our study. The dogs were used as control animals for toxicological studies by third-party researchers. Their animal experiment was approved by an Ethics Committee according to the Principles of Laboratory Animal Care (NIH publication no. 86-23, revised 1985) and the Swiss Regulations on Animal Experiments (Schweizerisches Tierschutzgesetz). The study approval number is BS 2197. This permission was not related to our study. The biopsies were taken from the thorax and flank immediately after euthanasia, fixed in either Histochoice (H2904; Sigma-Aldrich Chemie GmbH, Buchs, Switzerland) or 4% buffered formalin for 24 to 72 hr, processed, embedded in paraffin and cut as 4 μm sections. Specimens for RNA extraction were stored in RNAlater (AM7021; Ambion, Life Technologies, Zug, Switzerland).

RT-qPCR, Expression Cloning and Western Blot Analyses

RNA was extracted with RNeasy Fibrous Tissue Mini Kit (74704; Qiagen, Hombrechtikon, Switzerland) according to the manufacturer's instructions, and reverse transcribed into cDNA with reagents from Promega (M3681, N2511, U1515, C1181; Dübendorf, Switzerland). RT-qPCR was performed using the TaqMan Gene Expression Master Mix (4369016; Applied Biosystems, Life Technologies, Zug, Switzerland) with primers and probes listed in Supplemental Table 1.

TOPO cloning was performed according to the manufacturer's guidelines for the use of Champion pET Directional TOPO Expression Kit (K151-01; Invitrogen, Life Technologies, Zug, Switzerland). Recombinant V5-tagged canine proteins were expressed in BL21Star (DE3) Escherichia coli (K151-01; Invitrogen) after induction with IPTG (isopropyl β–D-thiogalactoside).

Bacterial pellets were lysed in lysis buffer (8 M Urea, 100 mM NaCl and 1 M Tris HCl, pH 8). Protein extraction from skin samples was carried out with 1% Triton X-100 lysis buffer [100 mM Tris HCl, pH 7.4, 150 mM NaCl, 1% Triton X-100, 10 mM NaF, 10 mM β-glycerophosphate, 10 mM Na_3VO_4, 1 mM PMSF and complete protease inhibitor EDTA-free (04693132001; Roche, Basel, Switzerland)] similarly to that

Table 1. Immunohistochemistry Protocols.

Antigen	Antigen Retrieval	Primary Antibody	Blocking	Visualization System	Chromogen	Washing Buffer
CD34	Target Retrieval Solution (S1699, Dako); 20 min at 80°C	Goat polyclonal CD34 antibody (sc-7045, LOT H2214, Santa Cruz Biotechnology) 1:50; overnight at 4°C	5% dried skim milk in PBS, pH 7.4; 1 hr at room temperature	LSAB+ Kit (K0679; Dako)	3-amino-9-ethylcarbazole (AEC+); 5 min at room temperature	TBS-T
Sox9	Tris-EDTA buffer, pH 9.0; 15 min in a pressure cooker	Rabbit polyclonal Sox9 antibody (sc-20095, LOT I1213, Santa Cruz Biotechnology) 1:150; 2 hr at room temperature	5% dried skim milk in PBS; 1 hr at room temperature	EnVision+ Kit (K4008; Dako)	AEC+; 10 min at room temperature	TBS-T
Keratin15	None	Mouse monoclonal Keratin 15 antibody (MS-1068-PABX, LOT 1068X1006A, Thermo Scientific) 1:1500; 1 hr at room temperature	4% bovine serum albumin in PBS; 1 hr at room temperature	EnVision+ Kit (K4004, Dako)	AEC+; 5 min at room temperature	PBS-T
LGR5	Sodium Citrate buffer pH 6.0; 20 min at 80°C	Rabbit polyclonal LGR5 antibody (HPA012530, LOT B83270, Sigma-Aldrich); 1:1200; 1 hr at room temperature	5% dried skim milk in PBS; 1 hr at room temperature	EnVision+ Kit (K4008, Dako)	AEC+; 10 min at room temperature	PBS-T
Nestin	Sodium Citrate Buffer pH 6.0; 25 min at 90°C; 15 min in absolute methanol	Rabbit polyclonal Nestin antibody (N1602, LOT 1C-307, IBL Int.); 1:200; overnight at 4°C	5% normal goat serum and 3% dried skim milk in PBS-T; 1 hr at room temperature	EnVision+ Kit (K4008, Dako)	AEC+; 10min at room temperature	PBS-T

Abbreviations: TBS-T, Tris-buffered saline with 0.05% Tween-20, pH 7.5; PBS, phosphate-buffered saline, pH 7.4; PBS-T, phosphate-buffered saline with 0.05% Tween-20, pH 7.4.

which has been described previously (Schulze et al. 2012). Equal amounts of total protein (bacterial lysate containing the recombinant proteins or skin extract) were subjected to SDS-PAGE and transferred onto polyvinylidene difluoride membranes. Signals were quantified using Odyssey Imaging System (LI-COR; Bad Homburg, Germany).

Method details are described in the Supplementary Information.

Immunohistochemistry

Detailed immunohistochemical (IHC) protocols used on paraffin sections can be found in Table 1. The epitopes recognized by the antibodies tested and used for IHC staining are provided in Supplemental Table 2. The protocol for the Nestin staining was kindly provided by K. Nishifuji, Tokyo University of Agriculture and Technology, Tokyo, Japan. All antibodies were diluted in Dako REAL™ Antibody Diluent (S2022; Dako, Baar, Switzerland). Indicated visualization systems were applied according to manufacturer's instructions (K0679, K4008 and K4004; Dako).

Prior to staining, the sections were deparaffinized and rehydrated by passage through xylene and graded alcohols. After IHC staining, sections were counterstained with Ehrlich's hematoxylin (4305; Merck, Zug, Switzerland). Consecutive sections were incubated with equal concentrations of normal goat, rabbit or mouse IgG (sc-2028, LOT A2913; sc-2027, LOT L1212; sc-2025, LOT H1512; Santa Cruz Biotechnology, Heidelberg, Germany) as negative controls (Supplemental Fig. 1). HC stages were assigned according to the criteria of Müntener et al. (2011).

Results

We first investigated the presence of mRNAs of the selected SC markers in canine skin using RT-qPCR. Ribosomal 18s was used as reference gene. Partial or full-length cDNAs of the corresponding transcripts bearing the epitope of antibodies to be tested for specificity and species cross-reactivity by western blotting were then cloned in *E. coli* and expressed as a V5-tagged fusion protein. V5 tag detection confirmed bacterial recombinant protein expression after

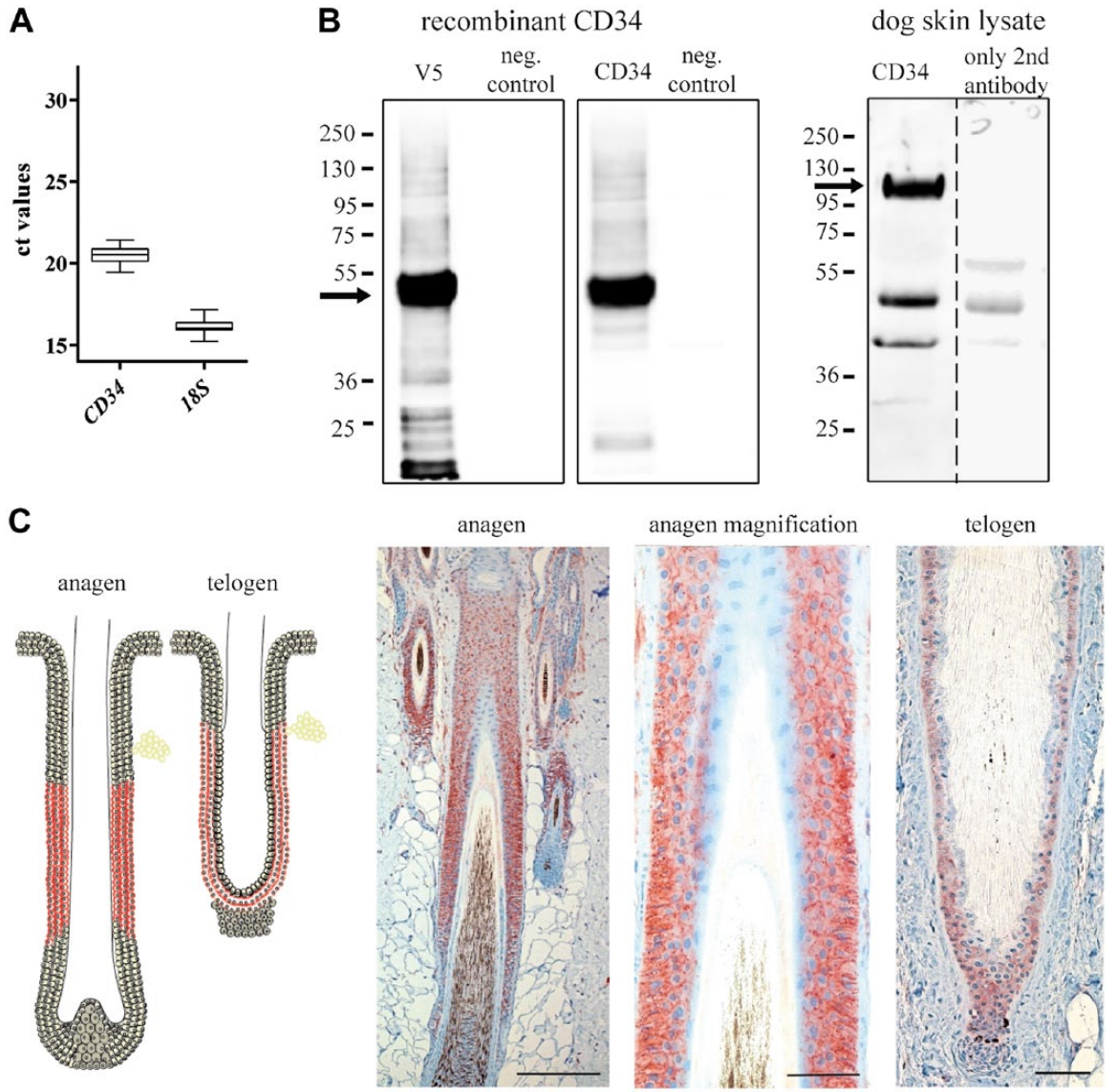

Figure 1. CD34. (A) RT-qPCR confirmed the presence of *CD34* mRNA in comparison to 18S rRNA; *n*=10. (B) Representative western blots. Left panel: Recombinant truncated V5-tagged CD34 was expressed in *E. coli* and lysates probed on the same blot with indicated antibodies. The negative control samples were collected from *E. coli* transfected with an empty vector without the gene fragment of interest. Anti-V5 and anti-CD34 antibodies detected the same band of about 50 kDa in size (calculated expected size: 51 kDa). Right panel: Dog skin lysates incubated with anti-CD34 antibody revealed the expected full-length protein band above 100 kDa, which was not detected when the anti-CD34 antibody was omitted. Note that both western blotting analyses were performed on the same membrane which was cut in half for incubations, as indicated with the dashed line. (C) Schematic drawing and immunohistochemical staining for CD34. Picture on the left: Anagen HF with positive staining in the ORS of the isthmus and the upper suprabulbar region. Picture in the middle: Magnification of the picture on the left. Note the membranous and cytoplasmic staining, which is most intense in the upper isthmus. Picture on the right: Telogen HF with fainter but positive staining in the ORS of the lower isthmus; *n*=5. Note that, for a better overview, the schematic drawings of the hair follicles depict only one follicle of each cycle stage in which a positive staining was observed. Scale (C, left) 100 µm; (C, middle) 25 µm; (C, right) 50 µm.

induction with IPTG. These protein samples served as a first test for antibody cross-reactivity. Subsequently, we examined canine whole-skin protein lysates to prove protein expression and to exclude hindered antigen detection of the antibodies by posttranslational protein modifications. After the confirmation that the chosen antibodies were most likely specific to detect the selected canine antigens, we established IHC staining protocols on formalin-fixed biopsies to identify the specific location of the SC-associated marker-expressing cells within the canine HF.

CD34

CD34 mRNA was detected and quantified in canine skin by RT-qPCR as shown in Fig. 1.

Truncated canine CD34 was expressed in *E. coli* for 4 hr after IPTG induction. Western blot analysis of bacterial lysate using a specific anti-V5 tag antibody revealed a band of about 50 kDa, which is in accordance with the calculated molecular weight of recombinant truncated CD34 (51 kDa; www.expasy.org). Similarly, the anti-CD34 antibody manufactured by Santa Cruz Biotechnology (sc-7045) recognized the same band representing recombinant canine CD34. Other antibodies tested were not specific (Supplemental Table 2). Supplemental Fig. 2 shows silver staining of a SDS polyacrylamide gel as a control for equal loading. A corresponding band of 100 kDa was observed when blotting canine whole-skin protein lysates, validating the use of this antibody for subsequent analyses.

Immunohistochemical staining of canine skin sections using the sc-7045 anti-CD34 antibody revealed a cytoplasmic-to-membranous signal in ORS cells of primary and secondary HFs. In the anagen HF, approximately two-thirds of the lower isthmic ORS and the upper suprabulbar region stained positively. In telogen HFs, the entire ORS was stained. However, staining in the telogen HF appeared less intense compared to the anagen ORS, as estimated by a semi-quantitative methodology; but the intensity increased towards the secondary germ, where it was most intense. Noteworthy, some telogen HFs were not stained at all by the anti-CD34 antibody and the basal membrane of the ORS keratinocytes was CD34-negative.

Sox9

Sox9 mRNA presence could be confirmed by RT-qPCR (Fig. 2).

Recombinant Sox9 protein fragment (containing the epitope recognized by sc-20095 Santa Cruz Biotechnology antibody) was detected with the V5 antibody. A band of about 20 kDa appeared more intense in IPTG-induced samples after 5 hr as compared to the uninduced *E. coli* (data not shown). The molecular weight of the observed band was slightly lower than the calculated molecular weight of 24 kDa (www.expasy.org). The sc-20095 anti-Sox9 antibody revealed a band of overlapping size (20 kDa) and an additional band of approximately 17 kDa representing potentially truncated proteins. When blotting canine skin lysate, two strong bands of around 55 kDa and 75 kDa were detected, which were much fainter when the first antibody was omitted. The calculated size of the full-length canine Sox9 is about 56 kDa.

On sections of canine skin, the sc-20095 anti-Sox9 antibody showed a scattered nuclear staining in the innermost layer of the ORS. Staining was most intense in the inferior portion and diminished from the suprabulbar region towards the infundibulum, where no cells were stained positively. Sox9 labeling was only observed in anagen III–VI HC stages. No positive staining was observed in anagen I and II or telogen HC stages.

Keratin15

The mRNA of the murine and human bulge marker *K15* was highly present in canine skin, as shown in Fig. 3.

Recombinant truncated K15 protein has a predicted molecular weight of 39 kDa (www.expasy.org). As shown in Fig. 3, the anti-V5 antibody detected several bands. A band representing the recombinant K15 fragment of around 39 kDa could be observed with both anti-V5 and anti-K15 (MS-1068-PABX, Thermo Scientific) antibodies 5 hr after IPTG induction. On whole-skin lysate, the secondary anti-mouse antibody detected a band of around 50 kDa, which likely corresponds to the non-specific detection of keratins, including the canine K15 protein (expected molecular weight, 55 kDa), also seen with other secondary antibodies (e.g., Fig. 1). In spite of this technical issue, we proved the specificity of the primary antibody through recombinant protein detection.

We observed K15 immunohistochemical staining in the cytoplasm of the entire ORS in the lower half of the isthmus in telogen HFs and in the ORS basal cell layer in the upper isthmus in anagen HFs. K15 also stained the basal cell layer of the epidermis (Supplemental Fig. 3).

LGR5

Canine *LGR5* mRNA was detected in canine skin, as shown in Fig. 4.

We failed to generate recombinant LGR5 protein; therefore, antibody specificity could not be confirmed. However, the antibody detected several bands, including one band of the expected size (94 kDa, www.expasy.org) in canine skin protein extract.

Anti-LGR5 antibody (HPA012530, Sigma-Aldrich) stained the cytoplasm of individual cells in the secondary germ of telogen and early anagen HFs only. Anagen III-VI HC stages did not show any positive staining cells.

Nestin

RT-qPCR analysis revealed *Nestin* mRNA presence in canine skin (Fig. 5).

We generated a truncated recombinant Nestin protein containing the epitope of the rabbit polyclonal anti-Nestin antibody manufactured by AbD Serotec (AHP1739). Analysis by western blotting of bacterial lysates 5 hr after IPTG induction using the anti-V5 and AHP1739 anti-Nestin antibodies revealed a band of approximately 25 kDa, which was in accordance with the calculated molecular weight (www.

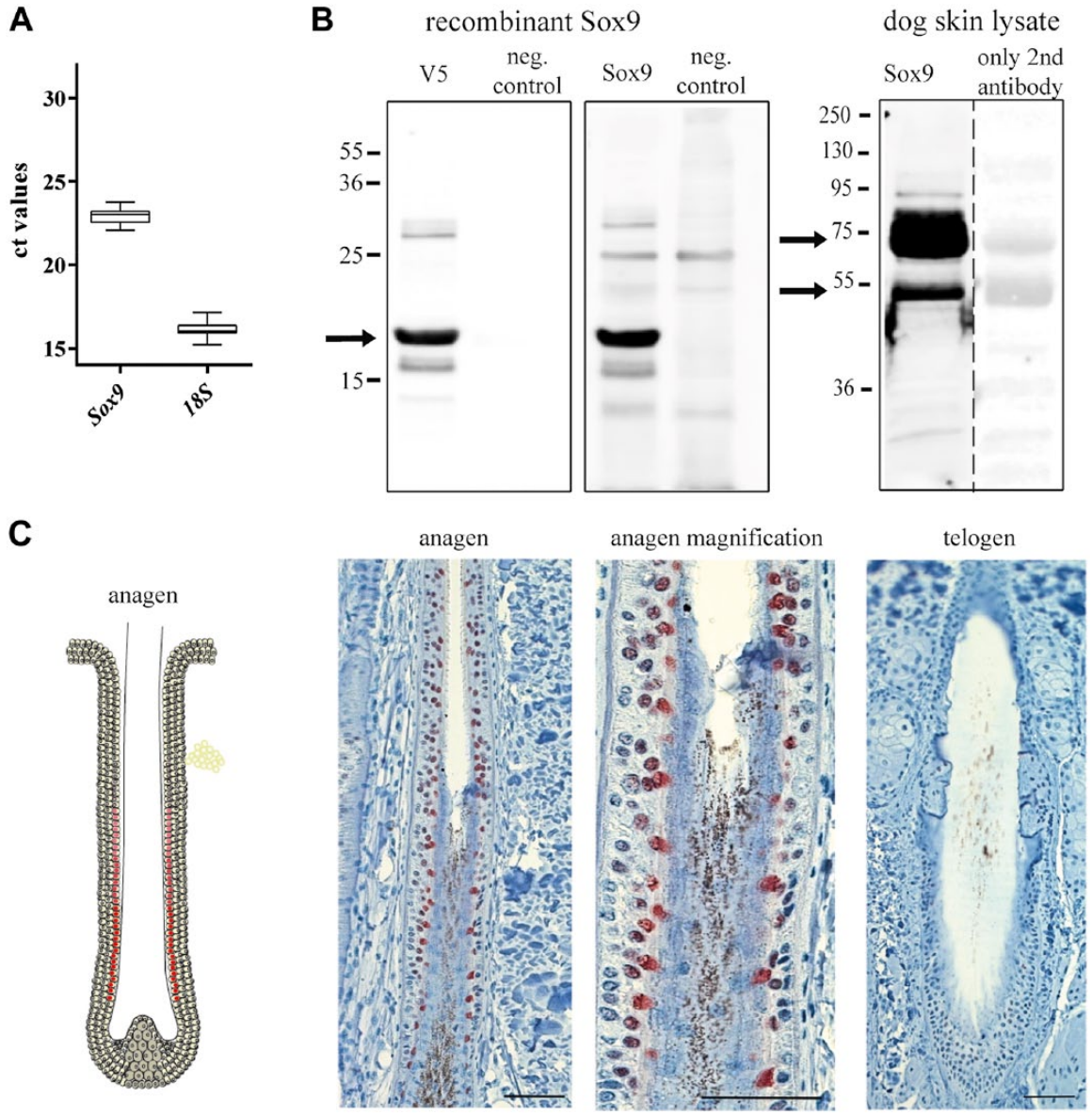

Figure 2. Sox9. (A) RT-qPCR confirmed the presence of *Sox9* mRNA in comparison to 18S rRNA; *n*=10. (B) Representative western blots. Left panel: Recombinant truncated V5-tagged Sox9 was expressed in *E. coli* and lysates probed on the same blot with indicated antibodies. The negative control samples were the same as in Fig. 1. Anti-V5 and anti-Sox9 antibodies detected a band corresponding to 20 kDa in size. The calculated size of the recombinant Sox9 protein fragment was 24 kDa. Right panel: Dog skin lysates probed with the same anti-Sox9 antibody revealed two strong bands of 55 kDa and 75 kDa, which were very faint when the anti-Sox9 antibody was omitted. Procedures were as per those specified in Fig. 1. (C) Schematic drawing and immunohistochemical staining for Sox9. Picture on the left: Anagen HF (representative HF for HC stages III-VI) with scattered and discrete positive staining in the innermost layer of the ORS. Picture in the middle: Magnification of the picture on the left. Note the nuclear staining. Picture on the right: Telogen HF. No positive staining was observed. *n*=5. Note that, for a better overview, the schematic drawings of the hair follicles depict only one follicle of each cycle stage in which a positive staining was observed. Scale (C, left) 50 µm; (C, middle) 25 µm; (C, right) 50 µm.

expasy.org). Santa Cruz Biotechnology (sc-21248) and IBL (N1602) anti-Nestin antibodies are directed against other epitopes and, accordingly, did not detect the recombinant protein; we were not able to express recombinant proteins containing these other epitopes in *E. coli*. Applying the antibodies to canine skin lysate, a band above 250 kDa could only be detected with N1602 IBL anti-Nestin antibody, whereas AHP1739 AbD Serotec and sc-21248 Santa Cruz antibodies only revealed nonspecific bands (data not shown).

With immunohistochemistry a distinct cytoplasmic staining of single cells within the dermal papilla and the connective tissue sheath surrounding the inferior portion of the

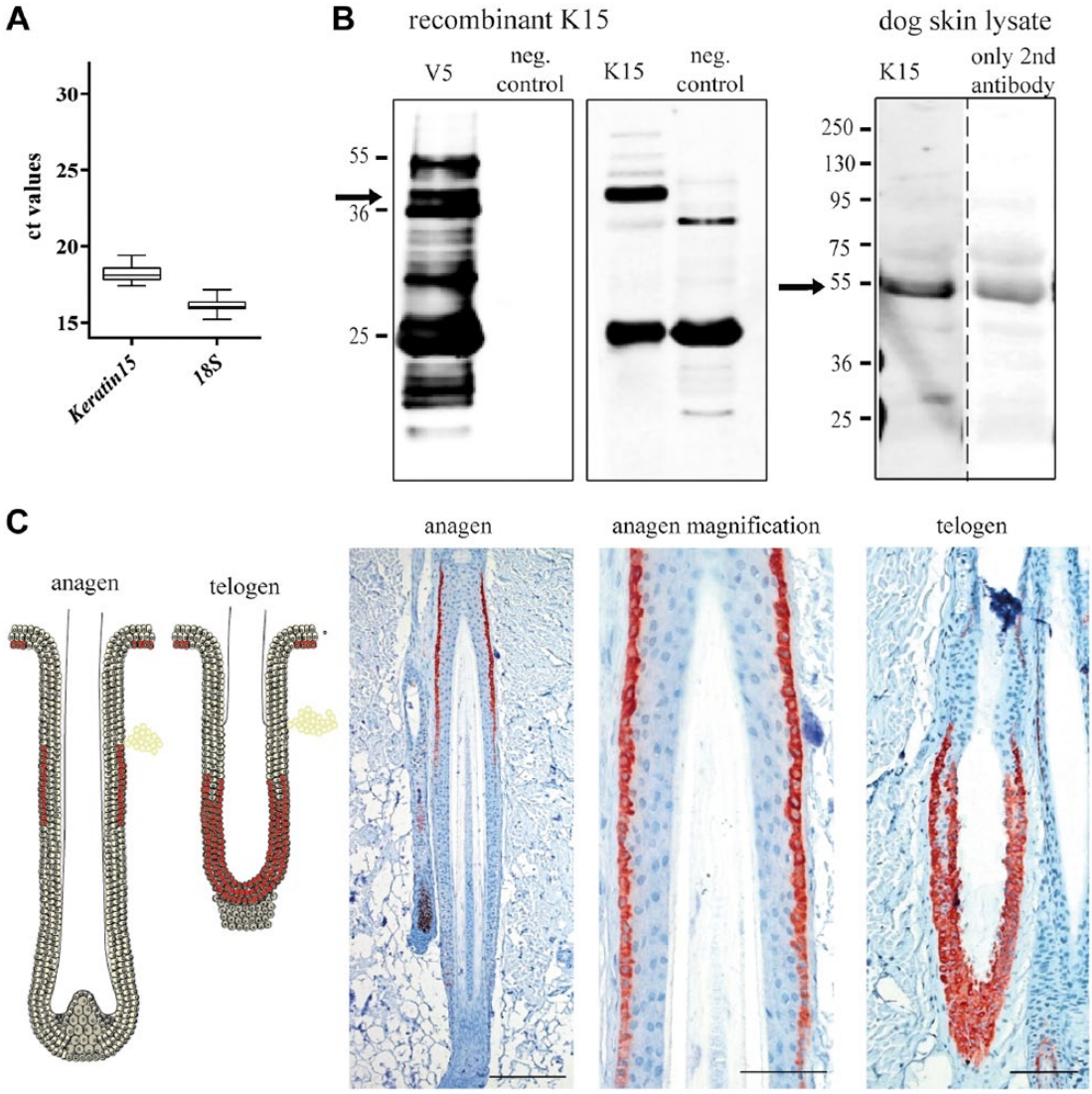

Figure 3. Keratin15. (A) RT-qPCR confirmed the presence of *K15* mRNA in comparison to 18S rRNA; *n*= 10. (B) Representative western blots. Left panel: Recombinant truncated V5-tagged K15 was expressed in *E. coli* and lysates probed on the same blot with indicated antibodies. The negative control samples were the same as in Fig. 1. Anti-V5 and anti-K15 antibodies detected the expected band of 39 kDa in size. Right panel: Dog skin lysates probed with the same anti-K15 antibody revealed a single band at the expected size of canine K15 of 55 kDa, which was also weakly detected with the secondary antibody alone. Procedures were as per those specified in Fig. 1. (C) Schematic drawing and immunohistochemical staining for K15. Picture on the left: Anagen HF with positive staining in the ORS basal cells of the upper isthmus. Picture in the middle: Magnification of the picture on the left. Note positive cytoplasmic staining. Picture on the right: Telogen HF with positive staining in the ORS of the lower half of the isthmus; *n*=5. Note that, for a better overview, the schematic drawings of the hair follicles depict only one follicle of each cycle stage in which a positive staining was observed. Scale (C, left) 100 µm; (C, middle) 25 µm; (C, right) 50 µm.

anagen HF was detected with the N1602 IBL antibody. In contrast, the two other antibodies did not reveal any specific labeling (data not shown). No positively stained cells were present in telogen HFs.

LGR6

Compared with the other examined genes, mRNA for canine *LGR6* was present at relatively low levels in canine skin (Fig. 6).

Using the anti-V5 antibody, a single band of 20 kDa with highest intensity after 24 hr IPTG induction could be seen in both induced (Fig. 6B) and uninduced (data not shown) lysates from *E. coli*. The molecular weight of this band was slightly lower than the calculated 26 kDa (www.expasy.org) of truncated LGR6 protein containing the epitope recognized by the rabbit polyclonal anti-LGR6 antibody from Santa Cruz Biotechnology (sc-99123) and was also observed with the anti-V5 antibody. Taking into account that both antibodies detect only one band of equal

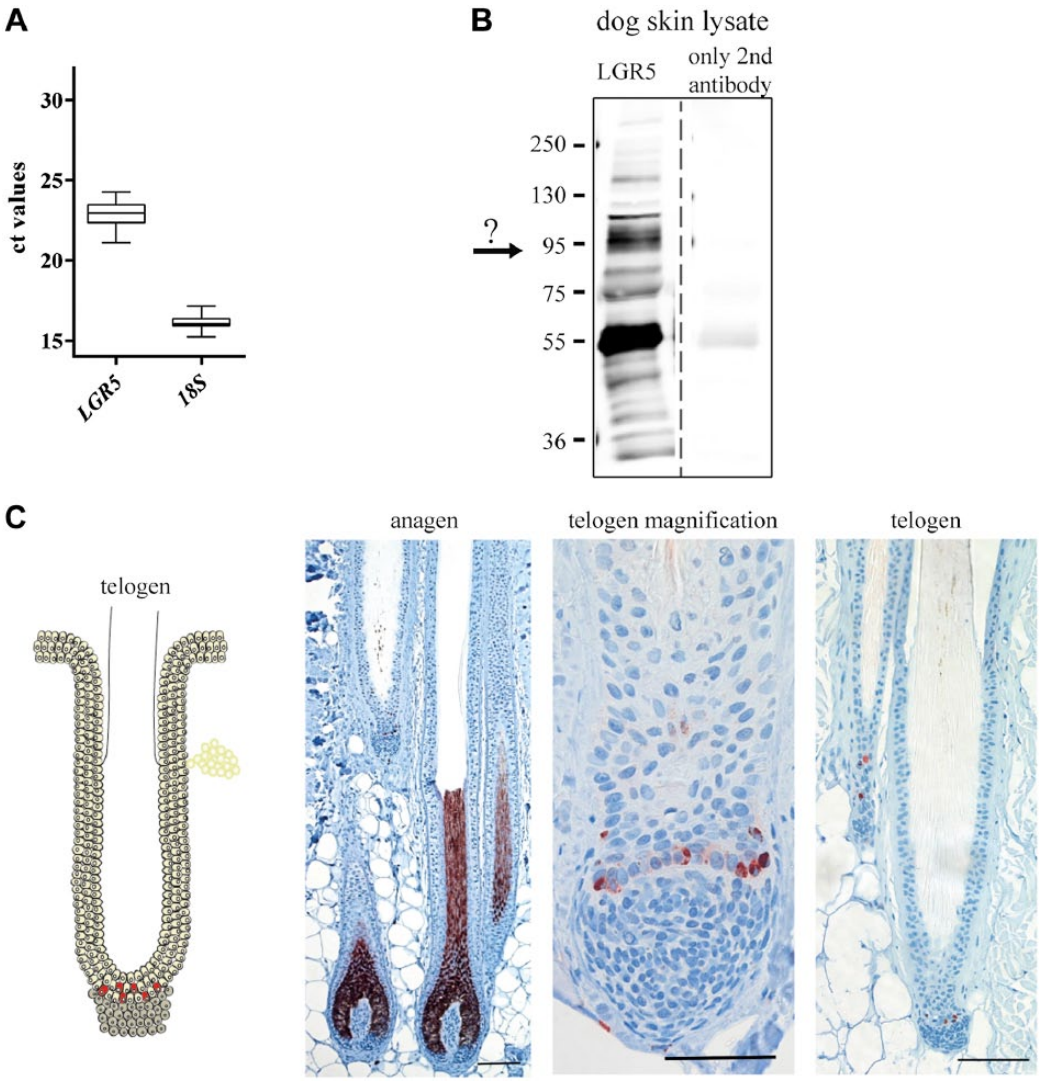

Figure 4. LGR5. (A) RT-qPCR confirmed the presence of *LGR5* mRNA in comparison to 18S rRNA; *n*=10. (B) Representative western blots. Note that we failed to generate recombinant LGR5 protein. Dog skin lysates probed with the anti-LGR5 antibody show several bands including a band of the expected size (94 kDa), which was not detected with the secondary antibody alone. Procedures were as per those specified in Fig. 1. (C) Schematic drawing and immunohistochemical staining for LGR5. Picture on the left: Late anagen HF. The cells did not show any positive staining in the entire HF. Picture in the middle: Telogen HF with positive staining of individual cells in the secondary hair germ. Note the cytoplasmic staining. Picture on the right: HF in the late telogen to anagen HC stage with positive individual cells in the secondary germ; *n*=5. Note that, for a better overview, the schematic drawings of the hair follicles depict only one follicle of each cycle stage in which a positive staining was observed. Scale (C, left) 100 µm; (C, middle) 25 µm; (C, right) 100 µm.

size, we consider the sc-99123 anti-LGR6 antibody to be specific. On canine skin protein lysate, we observed two bands at molecular weights of 95 kDa and 120 kDa that were most likely specific.

No specific immunohistochemical staining could be achieved with this antibody.

CD200

RT-qPCR confirmed the presence of *CD200* mRNA in canine skin (Fig. 7).

Expression of truncated CD200 protein negatively affected the bacterial growth compared to the *E. coli* transfected with plasmids carrying other SC marker genes, resulting in a lower OD_{600}. Application of the anti-V5 antibody on the recombinant protein samples did not reveal a band at the expected molecular weight of around 45 kDa (www.expasy.org,) but several unidentified bands were seen at 55, 36, 25 and below 15 kDa. The bands were weaker in the IPTG-induced samples as compared with the non-induced ones; strongest expression was observed after 4 hr without IPTG induction. We tested three anti-CD200

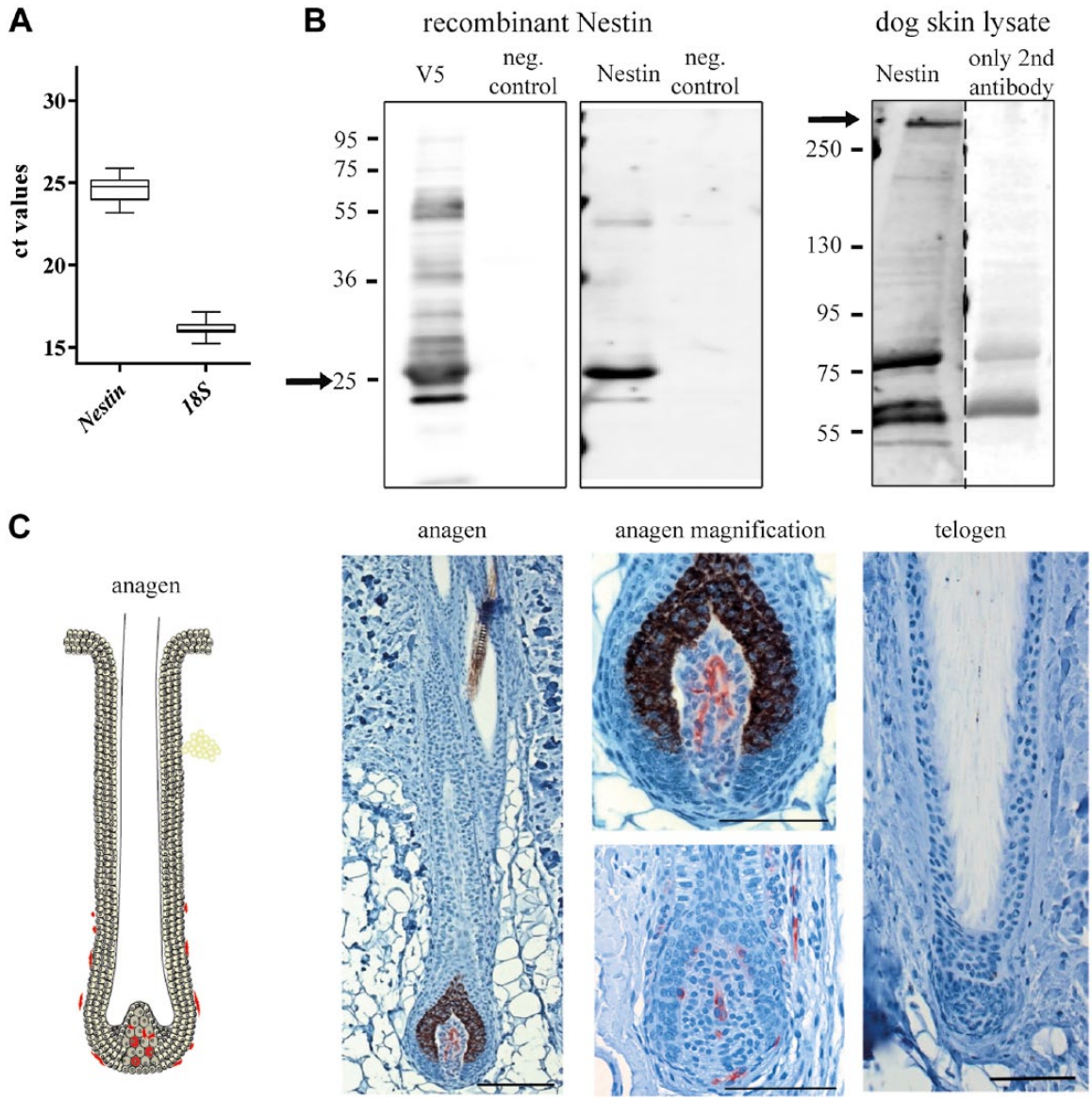

Figure 5. Nestin. (A) RT-qPCR confirmed the presence of *Nestin* mRNA in comparison to 18S rRNA; *n*=10. (B) Representative western blots. Left panel: Recombinant truncated V5-tagged Nestin was expressed in *E. coli* and lysates probed on the same membrane with indicated antibodies. The negative control samples were the same as that in Fig. 1. Anti-V5 and AHP1739 anti-Nestin (AbD Serotec) antibodies detected a band at 25 kDa in size. The expected size of the recombinant truncated Nestin protein is 22 kDa. Right panel: Dog skin lysates probed with N1602 anti-Nestin antibody (IBL) revealed a band above 250 kDa and two nonspecific bands of 55 and 75 kDa. Procedures were as per those specified in Fig. 1. (C) Schematic drawing and immunohistochemical staining for Nestin. Picture on the left: Anagen HF with scattered, positively stained cells within the dermal papilla. Picture in the middle: Magnifications of dermal papillae. Note the cytoplasmic staining of the dermal papilla and the connective tissue sheath. Picture on the right: Telogen HF. The cells did not show any positive staining in the entire HF; *n*=5. Note that, for a better overview, the schematic drawings of the hair follicles depict only one follicle of each cycle stage in which a positive staining was observed. Scale (C, left) 100 µm; (C, middle) 25 µm; (C, right) 50 µm.

antibodies (Supplemental Table 2); none of them detected a recombinant protein of the expected size expressed in *E. coli* or canine CD200 in skin protein lysate. Likewise, with immunohistochemistry, none of the three antibodies resulted in a specific staining of CD200+ cells in canine HFs. However, when applying the Aviva anti-CD200 antibody (ARP63444_P050) after antigen retrieval with pronase, an intense staining of the non-cornified Henle and Huxley layer of the inner root sheath, the infundibulum, the entire epidermis and the stratum corneum of the infundibulum, which is close to the epithelium, was observed (Supplemental Fig. 4).

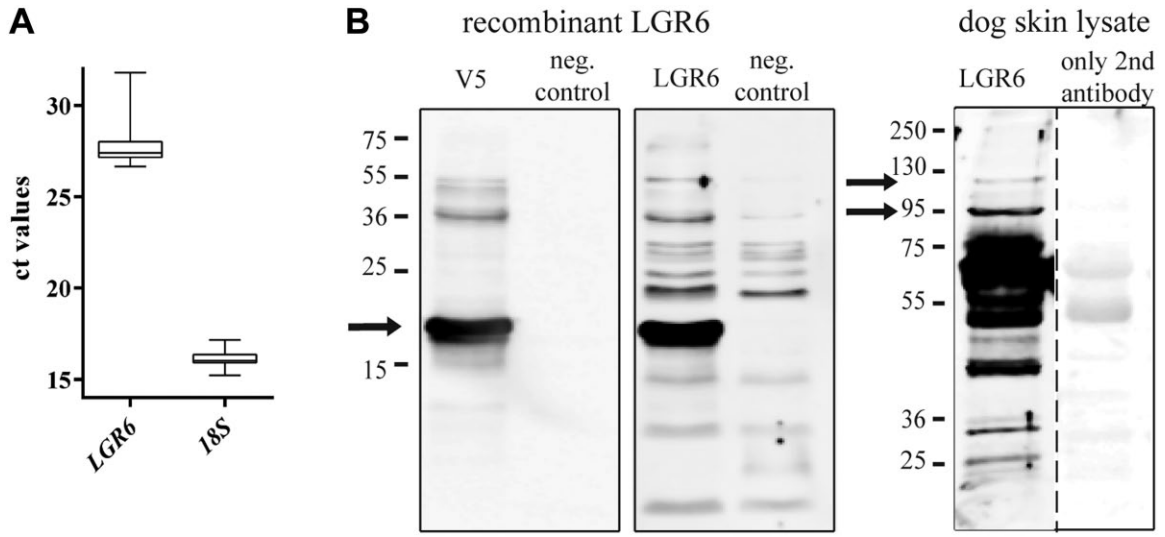

Figure 6. LGR6. (A) RT-qPCR confirmed the presence of *LGR6* mRNA in comparison to 18S rRNA; *n*=10. (B) Representative western blots. Left panel: Recombinant truncated V5-tagged LGR6 was expressed in *E. coli* and lysates probed on the same blot with indicated antibodies. The negative control samples were the same as in Fig. 1. Anti-V5 and anti-LGR6 antibodies detected a band of approximately 20 kDa. The expected size of recombinant LGR6 is 26 kDa. Right panel: Dog skin lysates incubated with anti-LGR6 antibody revealed two bands of 95 kDa and 120 kDa that were most likely specific for canine full-length LGR6 protein.

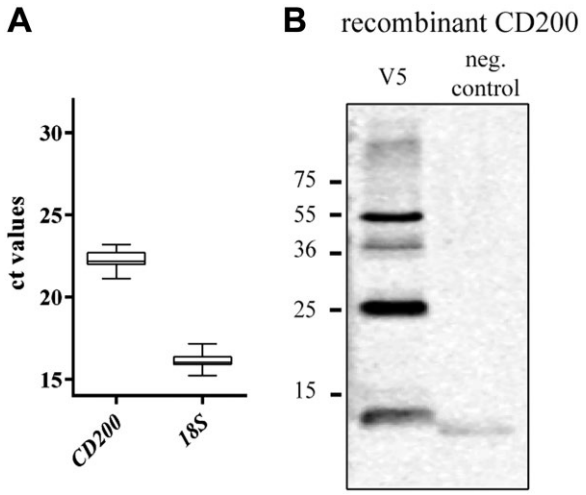

Figure 7. CD200. (A) RT-qPCR confirmed the expression of *CD200* mRNA in comparison to 18S rRNA; *n*=10. (B) Representative western blot of recombinant truncated V5-tagged CD200. The anti-V5 antibody detected several unidentified bands. The expected size of the recombinant CD200 protein fragment is 45 kDa.

Figure 8 shows a schematic drawing summarizing the locations of the investigated biomarkers observed by immunohistochemistry.

For simplification, in Figures 1 to 5 and 8, only individual anagen or telogen HFs of canine follicular compounds are shown in order to illustrate the observed staining pattern; follicular compounds in dogs may contain up to 15 follicles, each of which may cycle individually.

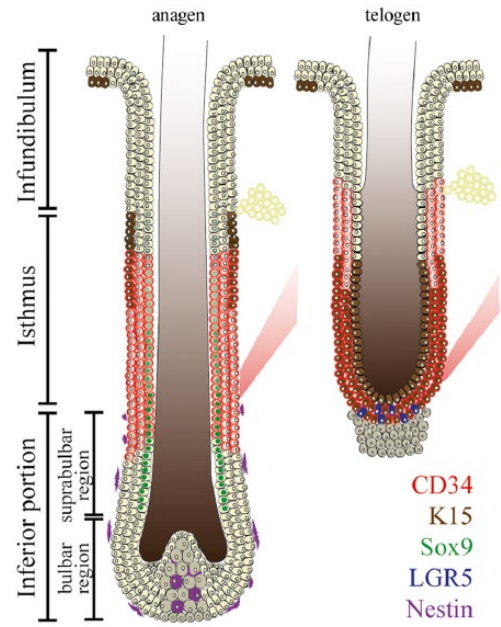

Figure 8. Proposed schematic overlay of the observed immunohistochemical staining in anagen and telogen HC stages. CD34+ and K15+ cells do not co-localize within the isthmus in anagen HFs but co-localize in telogen canine HFs. Sox9+ cells are present in the innermost layer of the anagen ORS and extend towards the CD34+ isthmic compartment. LGR5+ cells can be found solely in the secondary hair germ in telogen where CD34 and K15 are expressed as well. Nestin+ cells are detected only in the dermal papilla of the anagen follicle. Note that, for a better overview, the schematic drawings of the HFs depict only one follicle of each cycle stage in which a positive staining was observed.

An overview summarizing all tested antibodies can be found in Supplemental Table 2.

Discussion

The aim of our study was to further characterize the physiological SC compartment of canine HFs of healthy dogs. We tackled this goal in a comprehensive way using beagle dog samples and we are now able to present data based on qPCR, the expression of recombinant SC marker proteins, protein identification on western blots from whole-skin lysates, and, finally, the specific location for the selected markers within the HF.

The investigation of mRNA levels in canine skin confirms previous reports of *CD34, K15, Sox9, CD200* and *Nestin* mRNA presence in canine skin (Pascucci et al. 2006; Mercati et al. 2008; Kobayashi et al. 2009; Kobayashi et al. 2010; Brachelente et al. 2013). Furthermore, we demonstrated the presence of *LGR5* and *LGR6* mRNA, which has not been shown before.

In order to test the specificity and species cross-reactivity of the antibodies used for IHC labeling of the SC-associated biomarkers, we successfully expressed the recombinant protein carrying the relevant epitope for antibody detection for CD34, Sox9, K15, Nestin, LGR6 and eventually CD200. We furthermore identified the respective protein bands of CD34, Sox9, K15, LGR5, Nestin and LGR6 by western blot analysis in whole-skin lysates.

Having confirmed the specificity and the species cross-reactivity of the antibodies, we were able to establish IHC staining for CD34, Sox9, K15, LGR5 and Nestin. We were also able to demonstrate that certain antibodies fail to cross-react with the sought protein (a common hurdle in establishing immunostaining in species other than mice and human), and were therefore found unsuitable for the detection of the corresponding, naturally expressed canine protein.

On western blots of canine skin lysates, we observed a band of about 100 kDa using the anti-CD34 antibody; although, the molecular weight based on the amino acid composition of full-length canine CD34 is 51 kDa. Under the assumption that similar posttranslational modifications such as those that occur in mice and humans (Krause et al. 1994, Simmons et al. 1992) also occur in canine CD34 proteins, we consider the 100 kDa band detected by the sc-7045 anti-CD34 Santa Cruz Biotechnology antibody to be specific for canine CD34 protein. The observed staining pattern for CD34 in dogs is comparable to that in human tissue and in agreement with the reports of Kobayashi et al. (Trempus et al. 2003; Kloepper et al. 2008; Kobayashi et al. 2009), encompassing the isthmus and the suprabulbar regions of the inferior portion of the canine HF by sparing of the bulbar region. In addition to Kobayashi et al. (2009), we could demonstrate CD34 expression also in the telogen HF. Our results disagree with a report describing CD34 expression only in the basal cell layer of the ORS from the isthmus in canine HFs (Pascucci et al. 2006). The lack of positivity in the suprabasal cell layers in the latter report might be associated with the use of a different antibody or a different fixation or antigen retrieval procedure.

Sox9 protein expression in canine HFs has not been reported before. We were able to define a distinct nuclear staining of individual cells in the innermost layer of the anagen ORS, which is in agreement with the staining pattern in human and murine HFs (Vidal et al. 2005; Nowak et al. 2008; Fantauzzo et al. 2012). Investigating the canine whole-skin lysate, we detected two bands of 55 kDa and 75 kDa. The calculated molecular weight of canine Sox9 protein is around 56 kDa. We interpret the 75 kDa band either as a posttranslational modified form of Sox9 or a non-specific band. To further address this question, a $Sox9^{-/-}$ in vitro model would be useful.

In our study, we confirmed the presence of K15 mRNA, detected recombinant K15 by the MS-1068-PABX Thermo Scientific antibody, and demonstrated the presence of K15 in the ORS of the upper anagen isthmus and the lower telogen isthmus. Since the secondary anti-mouse antibody cross-reacted to some extent with proteins at the expected size of K15 in canine skin lysate, the MS-1068-PABX anti-K15 could not be conclusively validated for western blot analyses in these samples. Nevertheless, since the antibody specifically recognized the canine recombinant protein and our staining results are consistent with previously reported staining patterns in dogs (Kobayashi et al. 2009; Brachelente et al. 2013) as well as reports in human and mice (Trempus et al. 2003; Kloepper et al. 2008), we consider our immunohistochemistry staining to be specific for canine K15. The expression of K15 in canine telogen HFs has not been shown before. In humans, the basal cell layer of the epidermis is positive for K15 (Inoue et al. 2009), which is also the case for dogs.

This is the first report of LGR5 expression in canine HFs. We were able to identify *LGR5* mRNA in agreement with results demonstrated in human bulge cells (Garza et al. 2011). By IHC, we labeled LGR5+ cells in the secondary hair germ of telogen and early anagen HFs. This partially agrees with the observations of Jaks et al. (2008) in murine HFs; but, in mice, LGR5 was also detected in the lower ORS and the lower bulge in telogen and in the lower ORS during anagen. Unfortunately, no definitive conclusions can be drawn as to whether one of the identified bands on canine skin lysate western blots was specific because we lack a recombinant protein as a confirmation of the specificity of the antibody. However, the IHC staining was highly reproducible. Another approach to further determine canine LGR5 protein expression would be the generation of a $LGR5^{-/-}$ in vitro model. LGR5 is considered as a marker for rapidly cycling SCs. The fact that canine LGR5 was only detectable in telogen and early anagen HFs adds to the

hypothesis that LGR5 plays a role in the initiation of a new HC phase. Further research investigating the fate of LGR5+ cells during the canine HC will provide further functional insight.

Unlike Mercati et al. (2008), we labeled Nestin+ cells within the dermal papilla and the connective tissue sheath with the IBL anti-Nestin antibody (N1602). This staining pattern is in agreement with reports in human skin (Sellheyer and Nelson 2013). This antibody also detected a band of high molecular weight in canine skin lysates, which fits with the expected molecular weight because posttranslational modifications of canine Nestin protein might increase its size, as seen in mice (Sahlgren et al. 2001). In contrast, the AbD Serotec antibody (AHP1739) failed to identify canine Nestin in formalin-fixed skin sections or skin lysates, even though this antibody labeled the recombinant protein. Possible explanations for this circumstance could be either an inadequate antigen retrieval of the formalin-fixed tissue or the inaccessibility of the epitope due to posttranslational modifications. Sellheyer et al. (2011) described Nestin as a potential marker of mesenchymal SCs due to its location in the dermal papilla and the connective tissue sheath. Our results support their hypothesis and serve to study the canine mesenchymal SC compartment.

LGR6+ cells give rise to LGR5+ cells and contribute to HF regeneration (Rishikaysh et al. 2014) and thus LGR6 is considered as a marker for early SCs (Snippert et al. 2010). Human and murine LGR6 proteins are glycosylated, form disulfide bonds and appear around 100 kDa on western blots. We observed two different bands on our blots, and we presume that the canine LGR6 protein has a molecular weight of 95 kDa with an alternative form of 120 kDa because of similar modifications, as seen with the human and murine LGR6 proteins (www.uniprot.org). Although we could prove the specificity of the used antibody with a recombinant protein, we could not establish a positive IHC staining and thus the definite expression pattern of LGR6 in dogs still needs to be defined. This might be due to the fact that only few LGR6+ cells are present in the HF or that LGR6 is not expressed in all HC stages. This assumption is supported by the low *LGR6* mRNA expression levels. Another explanation for the negative staining results may again be the use of formalin-fixed tissue. The low expression level of *LGR6* suggests that, also in dogs, LGR6 is a marker for most primitive SCs as it is supposed in mice (Snippert et al. 2010).

We were not able to visualize CD200+ cells by IHC, which is in agreement with Kobayashi et al. (2010), who demonstrated the presence of mRNA but no positive staining. This negativity is most likely due to the fact that no canine specific antibody is available, based on our results testing the specificity and species cross-reactivity of three different antibodies. The anti-V5 antibody identified some bands that may represent truncated recombinant proteins, but none of the tested antibodies detected the recombinant proteins or a band on the skin protein lysate blots. The observed staining with the Aviva anti-CD200 antibody of the follicular inner root sheath (Huxley and Henle layer), the cornified layers of the infundibulum, and the entire epidermis has to be interpreted as a nonspecific staining artefact as the antibody should identify a transmembrane protein in bulge cells. Our observations therefore fail to confirm the report by Kobayashi et al. who demonstrated the isolation of CD200+ HF keratinocytes by FACS with the Serotec antibody (Ohyama and Kobayashi 2012).

In summary, we were able to establish specific IHC staining for CD34, Sox9, K15, LGR5 and Nestin. Like in humans, CD34+ staining can be found in the lower isthmus and the suprabulbar regions of the anagen HF (Kloepper et al. 2008). Sox9+ cells are present in the innermost layer of the anagen ORS, which is in agreement with findings in human and mice (Vidal et al. 2005; Krahl and Sellheyer 2010). Sox9+ cells seem to co-localize with CD34+ cells in the anagen HF. K15+ cells are present in outermost layer of the upper isthmus of the anagen HFs and in the entire ORS of the lower 2/3 of the isthmus in telogen follicles. In telogen HFs, K15+ cells seem to co-localize with CD34+ cells but not in anagen HFs. This staining pattern is in agreement with other reports in canine and some reports about the immunoreactivity in murine and human HFs (Lyle et al. 1998; Liu et al. 2003; Kobayashi et al. 2009). In telogen HFs, LGR5+ cells likely co-localize with CD34+ and K15+ cells but LGR5+ cells are not present in anagen HFs. The presence of LGR5+ cells in the secondary germ is in agreement with findings in mice (Jaks et al. 2008). Nestin is expressed within the mesenchymal compartment of the HF and thus does not co-localize with the other markers investigated in this study. Nestin+ cells are found in the same compartment as in human HFs (Sellheyer et al. 2011). Taken together, our results demonstrate that the canine SC-associated biomarker expression pattern resembles, in many aspects, the human HF SC compartment (CD34, K15, Sox9, Nestin). It also shares features with the murine SC reservoir (K15, Sox9, LGR5). Disagreement of marker expression occurs in terms of the lack of Sox9+ cells in canine telogen HFs and, compared to mice, the restriction of LGR5 expression to telogen and early anagen HC stages.

Our data will be essential to gain deeper insight into the SC biomarker profile in dogs and enable studies that explore, for example, changes within the SC compartment in different alopecic disorders. It will also help in the characterization of follicular organoids, which will facilitate functional studies in regard to the molecular pathways involved in SC activation and regulation. This knowledge is necessary to define alterations in the signaling cascades and the molecular SC signature in alopecic dogs. Only a thorough investigation of the disruption of the molecular signature in alopecia will enable the development of successful

causal therapeutic approaches. Furthermore, our data will also aid in evaluating the role of follicular SCs in the development of skin tumors and their progression. Preliminary data investigating the mRNA levels of the examined SC markers lead to the hypothesis that dogs with alopecic disorders like alopecia X or recurrent flank alopecia have pathological alterations in the HF SC compartment (Welle and colleagues; unpublished observations).

In addition, the investigation of the canine SC markers in skin disorders may also be of benefit for the disease counterpart in humans. As outlined above, dogs and humans share some properties regarding their HC, the SC-associated biomarker expression pattern and hormonal responses. Purba et al. (2014) have already summarized the major disadvantages of the murine model when studying human HF SCs. Our results may, in the future, also contribute to the understanding of human alopecia and skin cancer development, and our ongoing further investigations may help to find new therapeutic approaches for disorders associated with an impaired SC compartment.

Acknowledgments

We are grateful to Dr. J. Janzen, Histopathology and VascPath, Gümligen, Switzerland for providing human skin biopsies to test CD200 antibodies and to K. Nishifuji, Tokyo University of Agriculture and Technology, Tokyo, Japan for providing the anti-Nestin staining protocol. Furthermore, we would like to thank Ursula Sattler, Sebastian Rupp, Dr. Lisa Baumann, Manuela Bozzo, Erika Bürgi and Evelyne Rohrer for their precious technical support.

Authors Contributions

NMG performed the immunohistochemistry, molecular cloning and RT-qPCR experiments, analyzed the data and wrote the paper. BSS carried out the western blot experiments. FCO and AG supported the practical work with their expertise. EJM supported the study with her expertise and amended the manuscript. MMW designed the study, supervised the work, supported the study with her expertise and drafted the manuscript. DJW supervised the work, analyzed the data and drafted the manuscript.

Competing Interests

The authors declared no potential conflicts of interest with respect to the research, authorship, and/or publication of this article.

Funding

The authors disclosed receipt of the following financial support for the research, authorship, and/or publication of this article: This study was funded by the European Society of Veterinary Dermatology (ESVD) and the Spezialisierungskommission of the Vetsuisse Faculty, University of Bern, Switzerland.

References

Arwert EN, Hoste E, Watt FM (2012). Epithelial stem cells, wound healing and cancer. Nat Rev Cancer 12:170-180.

Barker N, van Es JH, Kuipers J, Kujala P, van den Born M, Cozijnsen M, Haegebarth A, Korving J, Begthel H, Peters PJ, Clevers H (2007). Identification of stem cells in small intestine and colon by marker gene Lgr5. Nature 449:1003-1007.

Brachelente C, Porcellato I, Sforna M, Lepri E, Mechelli L, Bongiovanni L (2013). The contribution of stem cells to epidermal and hair follicle tumours in the dog. Vet Dermatol 24:188-94.e41.

da Silva-Diz V, Solé-Sánchez S, Valdés-Gutiérrez A, Urpí M, Riba-Artés D, Penin RM, Pascual G, González-Suárez E, Casanovas O, Viñals F, Paramio JM, Batlle E, Muñoz P (2013). Progeny of Lgr5-expressing hair follicle stem cell contributes to papillomavirus-induced tumor development in epidermis. Oncogene 32:3732-3743.

Fantauzzo KA, Kurban M, Levy B, Christiano AM (2012). Trps1 and its target gene Sox9 regulate epithelial proliferation in the developing hair follicle and are associated with hypertrichosis. PLoS Genet 8:e1003002.

Garza LA, Yang CC, Zhao T, Blatt HB, Lee M, He H, Stanton DC, Carrasco L, Spiegel JH, Tobias JW, Cotsarelis G (2011). Bald scalp in men with androgenetic alopecia retains hair follicle stem cells but lacks CD200-rich and CD34-positive hair follicle progenitor cells. J Clin Invest 121:613-622.

Greco V, Chen T, Rendl M, Schober M, Pasolli HA, Stokes N, Dela Cruz-Racelis J, Fuchs E (2009). A two-step mechanism for stem cell activation during hair regeneration. Cell Stem Cell 4:155-169.

Hsu YC, Li L, Fuchs E. 2014. Transit-amplifying cells orchestrate stem cell activity and tissue regeneration. Cell 157:935-949.

Inoue K, Aoi N, Sato T, Yamauchi Y, Suga H, Eto H, Kato H, Araki J, Yoshimura K (2009). Differential expression of stem-cell-associated markers in human hair follicle epithelial cells. Lab Invest 89:844-56.

Jaks V, Barker N, Kasper M, van Es JH, Snippert HJ, Clevers H, Toftgård R (2008). Lgr5 marks cycling, yet long-lived, hair follicle stem cells. Nat Genet 40:1291-1299.

Kloepper JE, Tiede S, Brinckmann J, Reinhardt DP, Meyer W, Faessler R, Paus R (2008). Immunophenotyping of the human bulge region: the quest to define useful in situ markers for human epithelial hair follicle stem cells and their niche. Exp Dermatol 17:592-609.

Kobayashi T, Iwasaki T, Amagai M, Ohyama M (2010). Canine follicle stem cell candidates reside in the bulge and share characteristic features with human bulge cells. J Invest Dermatol 130:1988-1995.

Kobayashi T, Shimizu A, Nishifuji K, Amagai M, Iwasaki T, Ohyama M (2009). Canine hair-follicle keratinocytes enriched with bulge cells have the highly proliferative characteristic of stem cells. Vet Dermatol 20:338-346.

Krahl D, Sellheyer K (2010). Sox9, more than a marker of the outer root sheath: spatiotemporal expression pattern during human cutaneous embryogenesis. J Cutan Pathol 37:350-356.

Krause DS, Ito T, Fackler MJ, Smith OM, Collector MI, Sharkis SJ, May WS (1994). Characterization of murine CD34, a marker for hematopoietic progenitor and stem cells. Blood 84:691-701.

Li L, Mignone J, Yang M, Matic M, Penman S, Enikolopov G, Hoffman RM (2003). Nestin expression in hair follicle sheath progenitor cells. Proc Natl Acad Sci U S A 100:9958-9961.

Liu Y, Lyle S, Yang Z, Cotsarelis G (2003). Keratin 15 promoter targets putative epithelial stem cells in the hair follicle bulge. J Invest Dermatol 121:963-968.

Lyle S, Christofidou-Solomidou M, Liu Y, Elder DE, Albelda S, Cotsarelis G (1998). The C8/144B monoclonal antibody recognizes cytokeratin 15 and defines the location of human hair follicle stem cells. J Cell Sci 111(Pt 21):3179-88.

Maxie G (2015). 'Skin and Integument.' In Maxie G (ed.) Jubb, Kennedy & Palmer's Pathology of Domestic Animals. St Louis: Elsevier Saunders.

Mercati F, Pascucci L, Gargiulo AM, Dall'Aglio C, Ceccarelli P (2008). Immunohistochemical evaluation of intermediate filament nestin in dog hair follicles. Histol Histopathol 23:1035-1041.

Meyer W (2009). 'Hair follicles in domesticated mammals with comparison to laborytory animals and humans' in Mecklenburg L et al. (eds.) Hair loss disorders in domestic animals. Oxford: Wiley-Blackwell.

Müntener T, Doherr MG, Guscetti F, Suter MM, Welle MM (2011). The canine hair cycle - a guide for the assessment of morphological and immunohistochemical criteria. Vet Dermatol 22:383-395.

Nowak JA, Polak L, Pasolli HA, Fuchs E (2008). Hair follicle stem cells are specified and function in early skin morphogenesis. Cell Stem Cell 3:33-43.

Ohyama M, Kobayashi T (2012). Isolation and characterization of stem cell-enriched human and canine hair follicle keratinocytes. Methods Mol Biol 879:389-401.

Ohyama M, Terunuma A, Tock CL, Radonovich MF, Pise-Masison CA, Hopping SB, Brady JN, Udey MC, Vogel JC (2006). Characterization and isolation of stem cell-enriched human hair follicle bulge cells. J Clin Invest 116:249-260.

Pascucci L, Mercati F, Gargiulo AM, Pedini V, Sorbolini S, Ceccarelli P (2006). CD34 glycoprotein identifies putative stem cells located in the isthmic region of canine hair follicles. Vet Dermatol 17:244-251.

Pinkus H (1951). Multiple hairs (Flemming-Giovannini); report of two cases of pili multigemini and discussion of some other anomalies of the pilary complex. J Invest Dermatol 17:291-301.

Purba TS, Haslam IS, Poblet E, Jiménez F, Gandarillas A, Izeta A, Paus R (2014). Human epithelial hair follicle stem cells and their progeny: current state of knowledge, the widening gap in translational research and future challenges. Bioessays 36:513-525.

Rishikaysh P, Dev K, Diaz D, Qureshi WM, Filip S, Mokry J (2014). Signaling involved in hair follicle morphogenesis and development. Int J Mol Sci 15:1647-1670.

Rompolas P, Greco V (2014). Stem cell dynamics in the hair follicle niche. Semin Cell Dev Biol 25-26:34-42.

Rosenblum MD, Olasz EB, Yancey KB, Woodliff JE, Lazarova Z, Gerber KA, Truitt RL (2004). Expression of CD200 on epithelial cells of the murine hair follicle: a role in tissue-specific immune tolerance? J Invest Dermatol 123:880-887.

Sahlgren CM, Mikhailov A, Hellman J, Chou YH, Lendahl U, Goldman RD, Eriksson JE (2001). Mitotic reorganization of the intermediate filament protein nestin involves phosphorylation by cdc2 kinase. J Biol Chem 276:16456-16463.

Schneider MR, Schmidt-Ullrich R, Paus R (2009). The hair follicle as a dynamic miniorgan. Curr Biol 19:R132-142.

Schulze K, Galichet A, Sayar BS, Scothern A, Howald D, Zymann H, Siffert M, Zenhäusern D, Bolli R, Koch PJ, Garrod D, Suter MM, Müller EJ (2012). An adult passive transfer mouse model to study desmoglein 3 signaling in pemphigus vulgaris. J Invest Dermatol 132:346-355.

Scott DW, Miller WH, Griffin CE (2001). Structure and Function of the Skin. In: Muller and Kirk's Small Animal Dermatology, 6th Edition. WB Saunders, Philadelphia, pp. 1-70.

Sellheyer K, Nelson P (2013). The concept of the onychodermis (specialized nail mesenchyme): an embryological assessment and a comparative analysis with the hair follicle. J Cutan Pathol 40:463-471.

Sellheyer K, Nelson P, Patel RM (2011). Expression of embryonic stem cell markers SOX2 and nestin in dermatofibrosarcoma protuberans and dermatofibroma. J Cutan Pathol 38:415-419.

Simmons DL, Satterthwaite AB, Tenen DG, Seed B (1992). Molecular cloning of a cDNA encoding CD34, a sialomucin of human hematopoietic stem cells. J Immunol 148:267-271.

Snippert HJ, Haegebarth A, Kasper M, Jaks V, van Es JH, Barker N, van de Wetering M, van den Born M, Begthel H, Vries RG, Stange DE, Toftgård R, Clevers H 2010. Lgr6 marks stem cells in the hair follicle that generate all cell lineages of the skin. Science 327:1385-1389.

Trempus CS, Morris RJ, Bortner CD, Cotsarelis G, Faircloth RS, Reece JM, Tennant RW (2003). Enrichment for living murine keratinocytes from the hair follicle bulge with the cell surface marker CD34. J Invest Dermatol 120:501-511.

Vidal VP, Chaboissier MC, Lützkendorf S, Cotsarelis G, Mill P, Hui CC, Ortonne N, Ortonne JP, Schedl A (2005). Sox9 is essential for outer root sheath differentiation and the formation of the hair stem cell compartment. Current Biol 15:1340-1351.

Watt FM (2014). Mammalian skin cell biology: at the interface between laboratory and clinic. Science 346:937-940.

Watt FM, Jensen KB (2009). Epidermal stem cell diversity and quiescence. EMBO Mol Med 1:260-267.

Wu XJ, Zhu JW, Jing J, Xue D, Liu H, Zheng M, Lu ZF (2014). VEGF165 modulates proliferation, adhesion, migration and differentiation of cultured human outer root sheath cells from central hair follicle epithelium through VEGFR-2 activation in vitro. J Dermatol Sci 73:152-160.